The metal–insulator transition in lanthanum strontium vanadate

M Sayer, R Chen†, R Fletcher and A Mansingh‡

Department of Physics, Queen's University, Kingston, Ontario, Canada

Abstract. The electrical properties of $La_{1-x}Sr_xVO_3$ change from those of a semiconductor to those of a metal as x is increased, with a metal–nonmetal transition occurring at $x \approx 0.2$. This has been studied using AC and DC conductivity and thermopower measurements over a temperature range from 4 to 400 K. In pure $LaVO_3$, transport occurs via the excitation of holes from acceptor states 0.12 eV above the valence band. In doped material, V^{4+} states associated with Sr^{2+} ions constitute a broad band of filled hole traps with the conductivity changing from semiconducting to metallic when the Fermi level attains a mobility edge produced by Anderson localization in the valence band. Evidence for localization is found in AC conductivity and a temperature dependent activation energy at temperatures below 100 K. A temperature dependence $\sigma = \sigma_0 \exp(-B/T^{1/n})$, where $n \sim 4$, is interpreted in terms of a model in which the Fermi level occurs within a tail of states at the edge of the valence band. No evidence is found for polaron formation, but the frequency dependence of AC conductivity suggests that multiple site hopping, and possible cluster formation is of importance.

1. Introduction

Lanthanum strontium vanadate $La_{1-x}Sr_xVO_3$ ($0 < x < 0.4$) is a perovskite whose electrical properties change from those of a semiconductor to a metal as the strontium content is increased, with a metal–nonmetal (MNM) transition at about $x \sim 0.2$ (Dougier and Casalot 1970). The incorporation of Sr^{2+} ions in La^{3+} sites leads to the formation of V^{4+} ions in place of V^{3+} and an enhanced hole conduction in the system of vanadium 3d bands. Mott (1972) has suggested that this system is one in which extrinsic conduction occurs for small or zero values of x, but that as x is increased conduction occurs initially by hopping through localized states and then by band conduction in extended states. In the intermediate range of concentrations, disorder arising from the random distribution of Sr^{2+} and La^{3+} induces Anderson localization of carriers in the crystal (Anderson 1958), and the predictions of the Anderson model should apply (Mott and Davis 1971, Mott 1973). These predictions include an activation energy on the nonmetallic side of the transition which varies as $\epsilon \propto (x_0 - x)^{1.8}$ where x_0 is the concentration at the MNM transition (Abram and Edwards 1972), a temperature dependence of the form $\ln \sigma \propto 1/T^{\ddagger}$ at low temperatures, and an AC conductivity which is frequency dependent in the hopping region.

† on leave from the Department of Physics, Tel Aviv University, Tel Aviv, Israel.
‡ NRC–CIDA Research Associate; permanent address: Department of Physics and Astrophysics, Delhi University, Delhi 110007, India.

In this paper we examine the experimental justification for these suggestions regarding the conduction process in LaSrVO$_3$. The results suggest that while Anderson localization is of importance in the MNM transition, some of the properties derive from the form of the density of states function $N(E)$ rather than a straightforward application of the hopping theory proposed by Mott.

2. Experimental details

2.1. Material preparation

Strontium doped LaVO$_3$ was prepared as sintered polycrystalline discs from appropriate mixtures of lanthanum and strontium oxalates and V$_2$O$_5$. The starting materials were thoroughly mixed and ground for 30 minutes in an agate mortar, and then fired in a platinum crucible for 2 hours at 600°C under a 95% argon 5% hydrogen atmosphere. During this state V$_2$O$_5$ was reduced to V$_2$O$_3$, and water and CO$_2$ emanated from the oxalates. The resulting black powder was reground for 30 minutes in the agate mortar and then pressed into discs of $\frac{1}{2}$ inch diameter and $\sim$ 0·075 inch thick under a pressure of $\sim$ 4 ton cm^{-2}. The discs were finally sintered at approximately 2000°C in a molybdenum crucible heated by a high frequency induction furnace. A reducing Ar/H atmosphere was maintained around the crucible at all times. Mechanically strong and electrically reproducible polycrystalline material was obtained if the firing temperature was within 50°C of the nominal melting temperature of about 2050°C. Sintering times were generally of a few minutes duration. Microscopic examination showed that the materials were dense polycrystalline solids with some inter-crystalline voids.

The composition was evaluated using chemical analysis and x-ray fluorescence, the latter technique also revealing the presence of Mo from the crucible. Mo diffusion into the disc did occur in regions of contact, but this was removed prior to measurements by surface grinding. Powder camera x-ray diffraction studies showed a diffraction pattern characteristic of La$_{1-x}$Sr$_x$VO$_3$ (Kestigan *et al* 1957), and ^{51}V NMR indicated that a single crystalline phase was present.

2.2 Experimental

Samples for electrical measurements were cut into bars or discs and surface ground before use. Two and four terminal measurements were made using conducting silver paint contacts in order to determine the DC conductivity down to helium temperatures. Unguarded three terminal AC measurements showed good agreement with DC data in regions where no frequency dispersion was present, and there was no evidence of strong capacitative effects which would have indicated barriers. The Seebeck coefficient was measured in air by arranging for a temperature gradient to exist across the sample and measuring the resulting thermal EMF with a high impedance voltmeter.

3. Results

3.1. DC conductivity

The logarithm of the DC conductivity plotted as a function of inverse temperature is

shown in figure 1. The results are in substantial agreement which those of Dougier and Casalot (1970) at high temperatures, although in general, for a given composition our conductivities are slightly lower and our activation energies are slightly higher than those quoted in the earlier work, Dougier and Casalot give no experimental details or
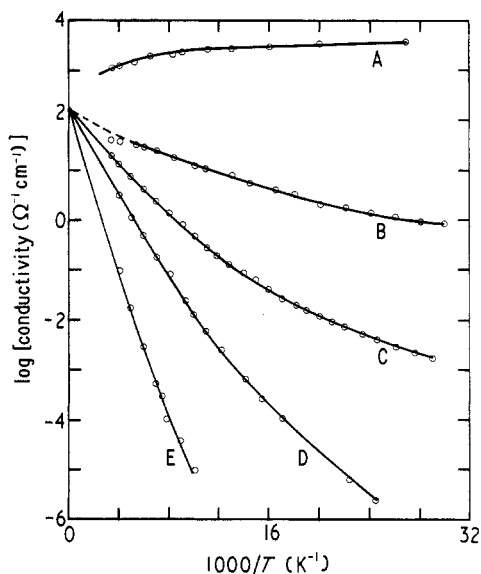

Figure 1. Log (conductivity) versus $1000/T$ for various compositions of $La_{1-x}Sr_xVO_3$. A: $x = 0.3$; B: $x = 0.2$; C: $x = 0.1$; D: $x = 0.05$; E: $x = 0$.
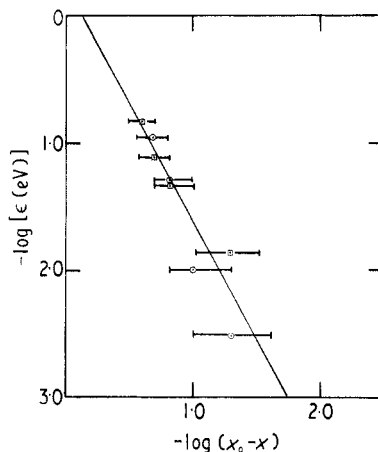
Figure 2. Log–log plot of the activation energy measured at 300 K versus $(x_0 - x)$ for $x_0 = 0.25 \pm 0.05$. The line $\epsilon = (x_0 - x)^{1.8}$ is drawn for $n = 1.8$ as predicted for an Anderson transition. Data points $\odot$ represent present work; $\square$ the data of Dougier and Casalot (1970) $(x_0 = 0.20)$.

analyses of their material and the differences may originate in the method of preparation. We have also recognised curvatures in the plots which were discounted in the earlier work. The conductivity shows a clear transition from an activated conductivity with an activation energy of 0.12 eV in undoped $LaVO_3$ to metallic characteristics for compositions with $x > 0.25$. A considerable uncertainty (± 0.05) exists in the value of x_0 corresponding to the transition. However, figure 2 shows that to this degree of accuracy the variation of the activation energy measured at 300 K with composition in the present work and by Dougier and Casalot (1970) can be represented by

$$\epsilon \sim (x_0 - x)^n \tag{1}$$

where $n = 1.8 \pm 0.5$ and $x_0 = 0.25$ for the present data. This variation is consistent with the predictions of the Anderson model for a MNM transition in a hopping conductor (Mott 1972). However, the uncertainty in the value of n is too large to discount other more general percolation models which lead to a value of $n \sim 1.6$ (Cohen 1971, Last and Thouless 1971, Kirkpatrick 1971) and this will be discussed later.

    If the conductivity $\sigma(T)$ at higher temperatures is described by an expression of the form

$$\sigma(T) = \sigma(0) \exp(-\epsilon/kT) \tag{2}$$

the intercept σ (0) on the conductivity axis has approximately the same value for all compositions, and σ (0) equals the conductivity of the composition corresponding to the MNM transition. Previous work (Dougier and Casalot 1970) has shown a maximum in conductivity at $T > 300$ K probably due to a decreasing mobility due to thermal
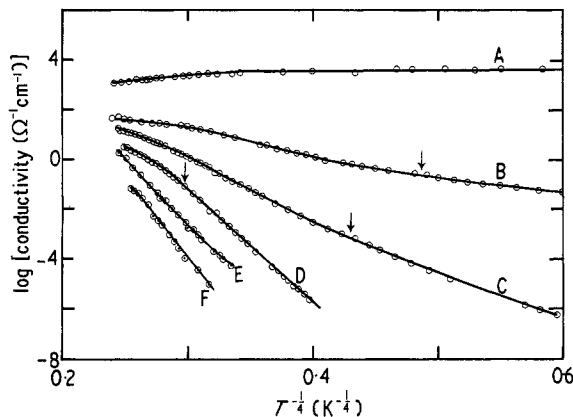

Figure 3. Fit of data to relation log σ_{10} versus $1/T^{\frac{1}{4}}$ as suggested for variable range hopping (Mott 1968). Data shown for several compositions. The arrows suggest the maximum temperature up to which the relation appears to be even approximately valid $T^{*}(T^{-\frac{1}{4}})$. Values for x are: A 0·3; B 0·2; C 0·1; D 0·05; E 0·02; F 0.

scattering. In the temperature range shown in figure 1 near 300 K, the extrapolation to $1000/T = 0$ leads to an approximate value of σ (0). The absence of a direct dependence of σ (0) on the concentration of trapping sites suggests that carriers are excited from localized acceptor levels to a band of states above a mobility edge in the valence band. In such a case, σ (0) should be the 'minimum metallic conductivity' defined by Mott (1968, 1973) as

$$\sigma_{\text{min}} = 0\cdot026 \, e^2/h^2 a \tag{3}$$

where the factor 0·026 is reduced from its earlier accepted value of 0·05 (Mott and Davis 1971) using a recent more stringent definition of the criterion for Anderson localization (Edwards and Thouless 1972). The parameter a is a measure of the carrier spacing at the MNM transition, and this may be estimated from the Sr^{2+} ion spacing for $x = 0\cdot25$ as ~ 8 Å. The conductivity calculated from equation 3 is $80 \, \Omega^{-1}\text{cm}^{-1}$ compared with the experimental value of $100 \, \Omega^{-1}\text{cm}^{-1}$.

At low temperatures, the curvature of the plots in figure 1 implies that the activation energy is temperature dependent. Following the suggestion of Mott (1972), the fit of the data to the expression for variable range hopping (Mott 1969)

$$\sigma \, (T) = \sigma_0 \exp \left(- \, B/T^{\frac{1}{4}} \right) \tag{4}$$

is shown in figure 3. A reasonable fit is obtained for a composition having $x = 0\cdot05$ at temperatures < 120 K. The fit is less appropriate for compositions of higher Sr^{2+} content, with the temperature range over which the fit is even approximately valid

moving to lower temperatures. Values for the parameters σ_0, B and the approximate onset temperature $T^*(T^{-\frac{1}{4}})$ for linear $T^{-\frac{1}{4}}$ behaviour for different compositions are given in table 1. The consistency of this functional relationship with other data will be examined later.

Table 1.

Composition x	$\sigma_0(T^{-\frac{1}{4}})$ $(\Omega^{-1}cm^{-1})$	B $(K^{-\frac{1}{4}})$	$T^*(T^{\frac{1}{4}})$ $(K)^{-\frac{1}{4}}$	$T^*(\text{AC})$ (K)
0	—	—	—	100
0·05	10^3	108	125	60
0·1	10^1	57	32	40
0·2	10^1	15	20	—

3.2. AC conductivity

The conductivity is shown as a function of inverse temperature and frequency for various compositions in figure 4. A frequency dependent AC conductivity is observed only below 100 K, with the onset temperature $T^*(\text{AC})$ (table 1) being similar to that for the possible $T^{-\frac{1}{4}}$ region. A substantial (exponential) temperature dependence is observed, this being least pronounced in pure $LaVO_3$ at the lowest temperatures.
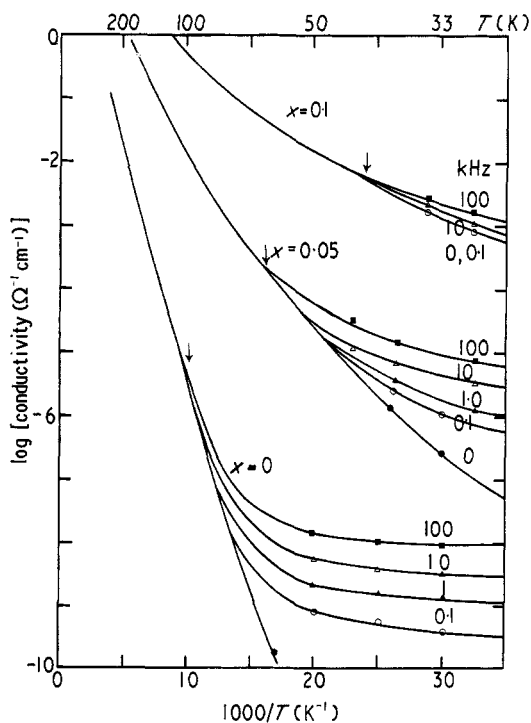

Figure 4. Conductivity as a function of $1000/T$ and frequency f(kHz) for various Sr^{2+} contents. Arrows indicate estimate of $T^*(\text{AC})$—the maximum temperature for which AC conductivity is observed.

The form of the frequency dependence for different compositions at approximately the same temperature is shown in figure 5. A power law of the form $\sigma \sim \omega^s$ is obtained with $s \sim 0.5$, s becoming smaller for the more metallic specimens. The dielectric constant (essentially κ_0) in the frequency range employed is in the range 25–40.
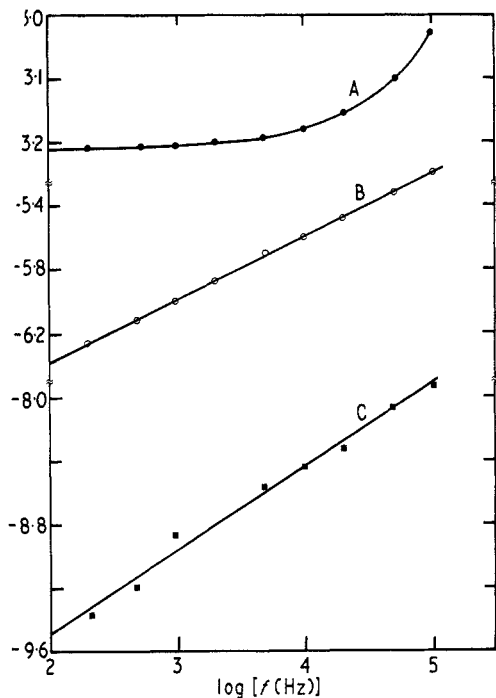

Figure 5. Composite diagram of conductivity as a function of frequency for three compositions at $T \sim 30\,\mathrm{K}$. The slope of the curve gives the parameter s in the relation $\sigma \sim \omega^s$. Curves A: $s \approx 0.38$, $x = 0.1$, $T = 28.5\,\mathrm{K}$; B: $s = 0.4$, $x = 0.05$, $T = 28.5\,\mathrm{K}$ C: $s = 0.52$, $x = 0$, $T = 33\,\mathrm{K}$.
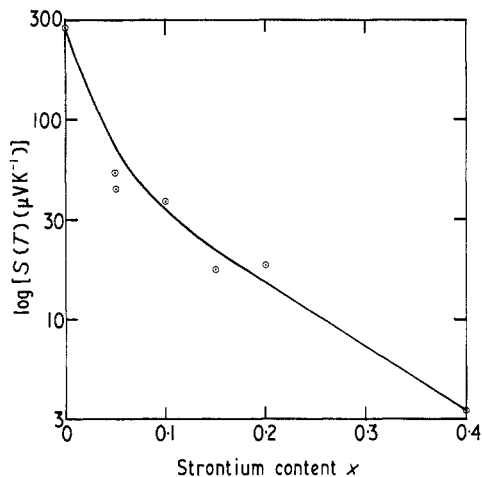

Figure 6. Seebeck coefficient $S(T) = \Delta E/\Delta T$ for various compositions of $La_{1-x}Sr_xVO_3$. Sign corresponds to p-type conduction at a measurement temperature of 300 K.

3.3. Seebeck coefficient

The sign of the thermopower corresponds to p-type conductivity and decreases with strontium content even before the nominal MNM transition. This is shown in figure 6. The dependence on temperature also changes as x increases, with pure $LaVO_3$ behaving like an extrinsic p-type semiconductor, the heavily doped materials acting as metals, and intermediate compositions having a relatively complex behaviour which is somewhat dependent on sample preparation, but in which the trend from semiconducting to metallic is observed consistently. The semiconductor and metallic types of behaviour are shown in figures 7(a) and (b) respectively. In the case of pure $LaVO_3$ (figure 7(a)), the results can be interpreted using the expression for extrinsic conduction with an activation energy ϵ (0) of magnitude

$$S(T) = \frac{k}{e}\left[\frac{\epsilon(0)}{kT} + A\right]$$

where A is a constant reflecting the scattering processes. The values obtained from the data of figure 7(a) are $\epsilon(0) \sim 0.12$ eV ± 0.005 eV and $A = \sim -0.6$. The negative value of A can arise in a crystalline system from a combination of scattering effects and an excitation energy which varies with temperature according to

$$\epsilon(T) = \epsilon(0) - \gamma T.$$

This results in a value of $A = r - \gamma/k$ where $r = 1$ for amorphous systems (Mott and Davis p 89), but $r \approx 2$–4 for crystalline systems. If LaSrVO$_3$ is taken to be a heavily

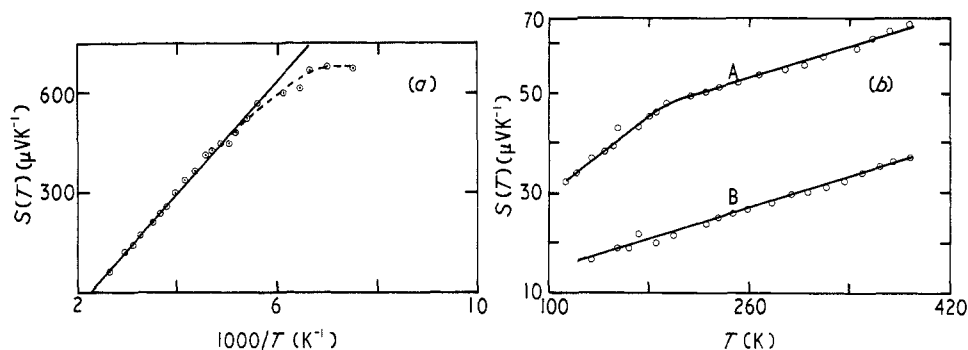Figure 7. Temperature dependence of the Seebeck coefficient for pure and Sr-doped LaVO$_3$. (a) $x = 0$; LaVO$_3$ ———O——— experimental data; ——— theory for $E = 0.12$ eV: (b) La$_{0.95}$Sr$_{0.05}$VO$_3$; ——— experimental data; A $x = 0.05$; B $x = 0.20$.

doped impurity semiconductor for which $r = 4$ (Tauc 1962), this results in a value of $\gamma = 5 \times 10^{-4}$ eV K^{-1}. This is small with respect to that calculated for amorphous semiconductors (Adler 1971) but is of the order of the value observed in systems such as InSb or Ge. At low temperatures in LaVO$_3$, the thermopower becomes less dependent on temperature. This change occurs in a temperature range where AC conductivity appears and it may be further evidence of carrier localization at these temperatures.

4. Discussion

4.1. Conduction mechanisms

Two models of the Anderson type could be used to interpret the MNM transition in LaSrVO$_3$. In one case, similar to doped Si or Ge, hopping occurs in a band of impurity states near the Fermi level and the MNM transition occurs when the Anderson criterion is satisfied. In the other case, if the Fermi level shifts from localized to extended states through a change in the uncompensated acceptor concentration, a MNM transition will occur when the Fermi level attains E_V, the energy corresponding to the mobility edge in the valence band. In general, the overall properties of LaSrVO$_3$ are more consistent with the second alternative.

If conduction occurs entirely within an impurity band, Mott (1969) has shown that a MNM transition should occur at an impurity concentration given by

$$n^{1/3}a_H \approx 0.27 \tag{7}$$

where a_H is the hydrogenic radius of the impurity state

$$a_H = h^2 \kappa_0 / me^2. \tag{8}$$

In LaSrVO$_3$ the MNM transition occurs when $n \sim 2 \times 10^{21}$ resulting in a value of a_H calculated from equation (7) of $2 \cdot 2$ Å. This value is less than an average ion spacing in the lattice and the situation is not that for which equation (7) was derived. In fact a wavefunction of this radius would imply strong polaron effects. An estimate of polaron hopping energies may be made by comparing the activation energies for high temperature conductivity and thermopower (Mott and Davis 1971 p118). For LaVO$_3$, both energies are $0 \cdot 12$ eV which implies that polaron effects are small and that the system behaves essentially as an extrinsic semiconductor. Other difficulties with an impurity band model for doped material include the large temperature dependence of AC conductivity and the relative insensitivity of the high temperature extrapolated conductivity σ (0) to the impurity concentration. We therefore examine the second alternative of a shift in the Fermi level towards the valence band.
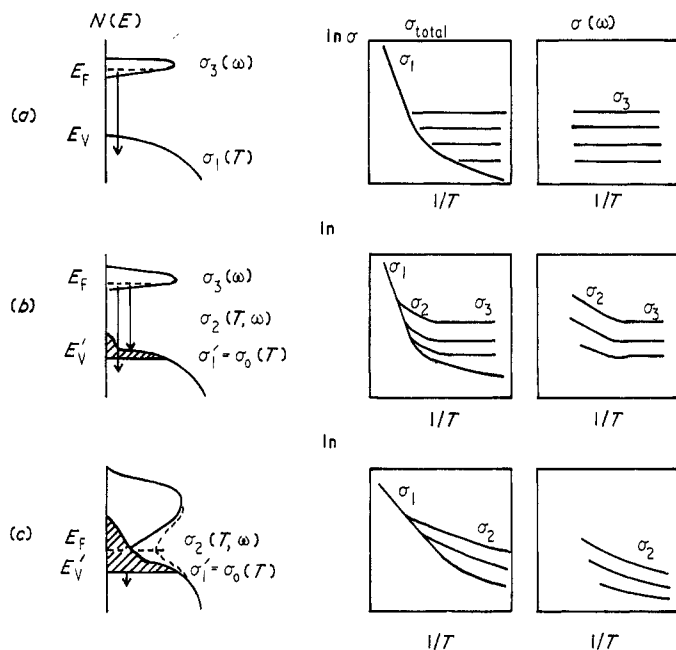

Figure 8. Possible density of states distribution $N(E)$ for lanthanum strontium vanadate and the resulting total and AC contributions to the conductivity. (a) excitation from partially filled impurity band to a conventional valence band; (b) partially filled impurity band, tail of localized states and mobility edge in the valence band; (c) broad impurity band overlapping tail of localized states on the valence band; minimum in the density of states near the Fermi level. σ_1 transport above mobility edge or in valence band, σ_2 hopping in localized states in valence band tail, σ_3 conduction directly between impurity states.

In order to interpret the temperature and frequency dependence, figure 8 illustrates various forms of the density of states $N(E)$ which are physically realistic for p-type conduction. In a conventional extrinsic semiconductor (figure 8(a)) conductivity σ_1 is independent of frequency and depends on temperature through the change in the number of carriers in the valence band $n_V = N_a \exp(\epsilon_1/kT)$. σ_3 corresponds to hopping conduction in a partly compensated impurity band (Pollak and Geballe 1961), which is weakly

dependent on temperature ($\sigma \sim T$) and has a frequency dependence $\sigma(\omega) \sim \omega^s$, where $0.7 < s < 1.0$. At low temperatures, variable range hopping should occur with a temperature dependence given by equation 4 (Mott 1969). In a disordered crystalline system, a tail of localized states is included extending from the valence band into the band gap (figure 8(b)). DC conductivity arises when carriers are excited into the band of states at the mobility edge, and the conductivity varies as $\sigma(T) = \sigma(0) \exp(-\epsilon_1/kT)$ where $\sigma(0)$ is the minimum metallic conductivity calculated using the Anderson criterion (Mott and Davis 1971 p200). Contributions to AC hopping arise from σ_3 as discussed previously and from σ_2 due to hopping in the tail of localized states in the valence band. σ_2 has a frequency dependence similar to that of σ_3, but a temperature dependence which is primarily due to the change in carrier concentration at the valence band edge. This occurs by excitation from lower impurity states and because of the energy distribution of initial and final states will lead to a temperature dependent activation energy with a mean value less than ϵ_1. Finally, in the case of heavy doping and large disorder energies (figure 8(c)), a broad band of fully compensated impurity states may overlap the tail of localized states in the valence band, leading to DC conductivity σ_1 at the mobility edge and hopping conduction σ_2 in the localized states between E_F and E_V. The form of the total density of states is shown as the dotted curve in figure 8(c). Since mixed conduction occurs, the variation of activation energy with composition will be complex and it will be difficult to distinguish between the behaviour expected for a simple Anderson model and that arising from general percolation effects. The observation of a relatively well defined $\sigma(0)$ and the trend in the transport properties through the MNM transition for LaSrVO$_3$ suggests that the model described by figure 8(c) is most appropriate. In this case, the variation of activation energy with composition arises more from percolation effects than from the Anderson theory.

4.2. The hopping régime

A major assumption in the preceding argument is that we are concerned with transport between pairs of sites associated with Sr^{2+} and separated by distance a. On this basis, Mott and Davis (1971 p42) show that for weak localization (carrier wavefunction radius $1/\alpha > a$), variable range hopping takes place and the constant B in equation 4 is given by

$$B = 2.1 \left[\alpha^3/kN(E) \right]^{\frac{1}{4}} \tag{9}$$

where $N(E)$ is the density of states at the Fermi level. Mott (1972) has discussed the temperature range below which localization should occur and the criteria developed can be used to obtain a value for α. For weak localization $\alpha a < 1$

$$kT^* > 1.5\epsilon_3(\alpha a)^3 \tag{10}$$

where ϵ_3 is the disorder energy influencing the hopping process, and the highest T^* occurs when $\alpha a = 1$. ϵ_3 may be estimated from the temperature dependence of the AC conductivity at the lowest temperatures. The values obtained from table 1 and figure 4 for $x = 0.05$ are $\epsilon_3 = 0.02$ eV, $T^* \approx 100$ K, leading to a value of $(\alpha a) \approx 0.7$. If a is taken as approximately equal to the Sr^{2+} spacing of 10 Å, $1/\alpha = 14$ Å. Substituting this value in equation (9) with $B = 108$ K$^{-\frac{1}{4}}$ gives a value of $N(E) \approx 6 \times 10^{17}$cm^{-3} eV^{-1}, while at higher Sr^{2+} concentrations, $N(E)$ increases by an order of magnitude. This value is small when compared to the Sr^{2+} concentration of 10^{20}cm^{-3} and implies either that

the interpretation in terms of pair hopping is suspect, or that the states are spread over a wide energy range with $N(E)kT \ll N_a$. An estimate of $N(E)$ by a different method is therefore desirable.

4.3. AC conductivity

The frequency dependence of AC conductivity in a hopping system has been examined by Pollak and Geballe (1961), Austin and Mott (1969) and Pike (1972), and a method of obtaining $N(E)$ from combined $T^{-\frac{1}{4}}$ plots and $\sigma(\omega)$ has been described by Haemers et al (1973). A similar procedure could be applied in the present work, but a limitation is found in the dependence on frequency. For example, the expression derived by Austin and Mott (1969)

$$\sigma(\omega) = 2 \cdot 9 \, e^2 k T n^2 \, [N(E)]^2 \, kT(\alpha^{-5}) [\ln (v/\omega)]^4 \tag{11}$$

has a frequency dependence of the form $\sigma(\omega) \sim \omega^s$, where $0 \cdot 7 < s < 1 \cdot 0$. Smaller values of s ($\gtrsim 0 \cdot 5$) can be extracted by making unphysical assumptions in equation (11) by assuming that the phonon frequency v is very small ($< 10^8$ Hz), but it is not possible to account for a constant value of s over 3–5 decades in frequency by this means. Values of $s < 0 \cdot 5$ are generally specifically excluded by the assumptions and approximations on which the models are based.

For lightly doped $La_{1-x}Sr_xVO_3$, the frequency dependence $\sigma \sim \omega^s$ has a value of $s < 0 \cdot 5$ and a pronounced temperature dependence and it is therefore difficult to interpret the behaviour in terms of single site hopping models. A value of $s < 0 \cdot 5$ has been observed in a few other systems, for example in VO_2 (Kabashima et al 1972, Sayer et al 1974) and has been predicted for AC conductivity involving multiple hops (Pollak 1965). In this case, paths containing different numbers of single site distances contribute to the AC conductivity, and the frequency dependence is weakened and the temperature variation is enhanced. Although quantitative estimates are difficult, the AC conductivity in $LaSrVO_3$ appears to be of this form with the AC properties determined by locally ordered chains of sites and the DC behaviour set by the uncorrelated regions surrounding such chains. These ordered regions cannot be of macroscopic dimensions since a frequency dependence of the Maxwell–Wagner–Sillars inhomogeneous loss form $\sigma(\omega) \sim 1/\omega$ would then arise. Cluster formation which may lead to the proposed behaviour has been discussed in general terms by Cohen and Jörntner (1974), while Mott (1974) has examined the effects of long range fluctuations just below the percolation threshold. Mott suggests that $\sigma(\omega) \sim f\omega/4\pi\epsilon$ where f is the volume of the sample in which the correlated behaviour occurs. Since f is a function of both ω and T, at any temperature, the correlated volume f will decrease with increasing frequency, thereby weakening the overall frequency dependence as observed in $LaSrVO_3$.

4.4. N(E) and thermopower S(T)

The data shown in figure 4 have been plotted as a $f(T^{-\frac{1}{4}})$ in order to facilitate comparison with Mott's theory of variable range hopping. However, a more general relation $\ln \sigma \sim D T^{-1/n}$ applies in other circumstances. Croitoru et al (1971) and Reyes (1975) have shown that a power law applies when the Fermi level lies within an extensive band tail of localized states, where the mobility is only weakly dependent on temperature, but $N(E)\mu(E)$ increases rapidly with $(E_F - E)$. Adler et al (1973) and Pollak (1972) have discussed percolation effects in systems where band tails of different forms exist. For a

general distribution where $N(E) \sim E^p$, Pollak (1972) gives

$$\ln \sigma \sim T^{-(p+1)/(p+4)} \tag{12}$$

and the proposed density of states for $LaSrVO_3$ shown in figure 8(c) is consistent with a $T^{-1/n}$ dependence arising from such a source.

The thermopower provides further justification for such a model. Cutler and Mott (1969) have interpreted the thermopower in a hopping semiconductor using the expression

$$S = \frac{-\pi^2}{3} \frac{k^2 T}{e} \left[\frac{\mathrm{d}\ln\sigma}{\mathrm{d}E} \right]_{E=E_F}. \tag{13}$$

If $kT \ll E_c - E_F$

$$\sigma = e\mu(E_F)\, N(E_F)\, kT$$

and

$$\mu(E) = \mu_0(E) \exp\left(-\omega(E)/kT \right).$$

By substitution

$$S = -\frac{\pi^2 k}{3e} kT \frac{\mathrm{d}\ln(\mu_0 N)}{\mathrm{d}E} - \frac{\mathrm{d}\omega}{\mathrm{d}E}. \tag{14}$$

This is of the form $A + ET$ and may be compared to the experimental results in figures 6 and 7(b). The rapid decrease in S with composition (figure 6) is consistent with the movement of the Fermi level through a band tail and into a band where $\mathrm{d}/\mathrm{d}E\,(\ln(\mu N(E)))$ is less rapidly varying. The temperature range of the thermopower measurements in figure 7 did not attain that where $T^{-\frac{1}{4}}$ or frequency dependent AC hopping was observed. For compositions with $x = 0{\cdot}05$ and $0{\cdot}2$, the intercepts on the S axis of 30 and $8\mu V\,K^{-1}$ respectively lead to values of $\mathrm{d}W/\mathrm{d}E$ in the range $0{\cdot}1$–$0{\cdot}03$. By comparison Cutler and Mott (1969) find values $0{\cdot}13$–$1{\cdot}6$ for Ce_2Se_4 in which hopping transport is better defined. This does suggest that the hopping mobility W is not a strong $f(E)$ in $LaSrVO_3$, particularly as the Fermi level approaches the mobility edge. From the slope $\mathrm{d}S\,\mathrm{d}T$, $\mathrm{d}/\mathrm{d}E$ (ln $(\mu N) \sim 4\,eV^{-1}$) over most of the range at higher temperatures. This is the value obtained only for the highest conductivities by Cutler and Mott (1969) and again is consistent with a small variation of (μN) with E. Further measurements at lower temperatures would be of interest but, in general, the thermopower is consistent with that expected for transport in a band of states above a mobility edge. One difficulty is that at higher temperatures in lightly doped material (say $x \sim 0{\cdot}05$) the thermopower should change from metallic to semiconducting as the proportion of carriers excited to the mobility edge increases. However if $N(E_F)$ is large and energy dependent, $S(T)$ may be dominated by structure in the density of states near the Fermi level. The relatively large effect of preparation conditions at intermediate compositions would support this view.

Finally, Dougier and Casalot (1970) have measured the magnetic susceptibility as a function of composition and have shown that the susceptibility decreases with increasing Sr^{2+} content. Since the total susceptibility will be the sum of contributions from localized states and carriers in extended states, on the present model, the susceptibility will be expected to decrease as the Fermi level rises through the tail of localized states and the small Pauli susceptibility of extended state carriers in the valence band becomes dominant. However, the magnetic properties require further work. S L Segel (1974, private communication) has shown that the linewidth of the ^{51}V NMR resonance line is very broad

(≈ 100 G), but tends to become narrower as x increases. This is the behaviour expected as carriers change from strongly localized to valence band states. with the original linewidth being due to interaction with strongly localized moments. Further work on this aspect of $LaSrVO_3$ is proceeding.

5. Conclusion

The transport properties of $La_{1-x}Sr_xVO_3$ show little evidence of polaron localization and bear a strong resemblance to those of a highly degenerate semiconductor. The MNM transition is associated with the movement of the Fermi level through a tail of localized states in the valence band until it attains the energy associated with a mobility edge. The latter appears to arise from localization of the Anderson type, and the magnitude of the conductivity at the transition is compatible with an Anderson model. The effects of localization are observed in AC conductivity and a temperature dependent activation energy at temperatures < 100 K. However, the simple models of variable range hopping often associated with a conductivity which varies as $\ln \sigma \sim B/T^{\frac{1}{4}}$ may not be applicable to highly conducting systems such as lanthanum strontium vanadate. The temperature dependence of the activation energy arises from carrier excitation from the Fermi energy into a tail of states at the edge of the valence band.

Acknowledgments

References

Abram R A and Edwards S F 1972 *J. Phys.* C: *Solid St. Physics* **5** 1183
Adler D 1971 *Amorphous Semiconductors* (Cleveland, Ohio: CRC Press)
Adler D, Flora P F and Senturia S D 1973 *Solid St. Commun.* **12** 9
Anderson P W 1958 *Phys. Rev.* **109** 1492
Austin I G and Mott N F 1969 *Adv. Phys.* **18** 41
Cohen M H 1971 *Phys. Today* **24** 26
Cohen M H and Jörntner J 1974 *Proc. 5th Conf. on Amorphous and Liquid Semiconductors* (London: Taylor and Francis) vol 1 p167
Croitoru N, Popescu C, Telnic M and Vescan L 1971 *Phys. Stat. Solidi* (b) **48** 429
Cutler M and Mott N F 1969 *Phys. Rev.* **181** 1336
Dougier P and Casalot A 1970 *J. Solid St. Chem.* **2** 396
Edwards J T and Thouless D J 1972 *J. Phys.* C: *Solid St. Phys.* **5** 807
Haemers J, Baetens E, and Vennik J 1973 *Phys. Stat. Solidi* (a) **20** 381
Kabashima S, Goto T, Nishimura K and Kawakubo T 1972 *J. Phys. Soc. Japan* **32** 158
Kestigan M, Dickinson J G and Ward R 1957 *J. Amer. Chem. Soc.* **79** 5598
Kirkpatrick S 1971 *Phys. Rev. Lett.* **27** 1722
Last B J and Thouless D J 1971 *Phys. Rev. Lett.* **27** 1719
Mott N F 1968 *J. Non-cryst. Solids* **1** 1
——1969 *Phil. Mag.* **19** 835
——1972 *Adv. Phys.* **21** 785

——1973 *Electronic and Structural Properties of Amorphous Semiconductors: 13th Scottish Universities Summer School in Physics* (London: Academic Press) p1
——1974 *Phil. Mag.* **29** 613
Mott N F and Davis E A 1971 *Electronic Processes in Non-Crystalline Materials* (London: Oxford UP)
Pike G E 1972 *Phys. Rev.* **B 6** 1572
Pollak M 1965 *Phys. Rev.* **138** 1822
——1972 *J. Non-cryst. Solids* **11** 1
Pollak M and Geballe T H 1961 *Phys. Rev.* **122** 1742
Reyes J M 1975 *Solid. St. Commun.* to be published
Sayer M, Mansingh A, Chen R and Reyes J M 1975 *Can. J. Phys.* to be published
Tauc J 1962 *Photo and Thermoelectric effects in semiconductors* (Oxford: Pergamon)